2014 International Joint Conference on Neural Networks (IJCNN)
July 6-11, 2014, Beijing, China

A New Fuzzy Shape Context Approach Based on Multi-clue and State Reservoir Computing

Zhidong Deng*, Kelaiti Xiao, and Jing Huang
State Key Laboratory of Intelligent Technology and Systems
Tsinghua National Laboratory for Information Science and Technology
Department of Computer Science
Tsinghua University
Beijing, China
Email: michael@tsinghua.edu.cn, {xklt11, huangijng10}@mails.tsinghua.edu.cn

Abstract—**This paper first builds a rule-based fuzzy representation of shape context and then present a multi-clue based fuzzy shape context approach (MFSC) using combination of geometric information and graph transduction. The MFSC takes complexity of object shape into account. In this approach, the distance between arbitrary two sampled points on any shape is redefined and graph transduction is used to correct and compensate training error. Furthermore, we propose a new fuzzy shape context approach based on both multi-clue and state reservoir computing. The experimental results show that the accuracy of detection achieved by our new approach on Kimia-216 and Kimia-99 datasets reaches up to 99.35% and 98.56%, respectively, which outperforms that of all the state-of-the-art shape context approaches.**

I. INTRODUCTION

Human being has powerful capabilities of simplifying and screening object in a visual object recognition task. In most cases, any object can be identified once one has a glimpse of external contour or shape of object. It is really in accord with the so-called edge priority theory supported by a lot of experimental results from cognitive psychology. In fact, shape features, instead of color ones, are often less affected by change in translation, rotation, and scaling, and have a faster response.

Using shape invariant features of object, Belongie et al. propose a shape context-based approach in 2000 [1], [2]. In this approach, any object is represented as a set of target sampled points. Each of the points is randomly picked as the origin of the log-polar coordinate frame and all the other sampled points on a shape are then projected to the log-polar frame. Moreover, the *K*-bin normalized histogram can be readily yielded. For arbitrary two different shapes, the cost function of matching all the sampled points is computed according to all the resulting histograms at the points. Using the Hungarian method, the maximum bipartite matching can be done and the similarity between the two shapes is evaluated. In 2005, Mori et al. present a generalized shape context approach [3], which considerably improves the matching precision through replacing the original sampled points with tangent vector components. The shape classification approach using the inner-distance is presented in 2007 [4]. The inner-distance more reasonably expresses the distance between two sampled points through the use of the closed curve graph information. In 2010, Bai et al. propose a graph transduction approach for learning context-sensitive shape similarity [5]. This approach constructs the graphs of all the samples of the same class of object and some of the detection errors are then corrected using the transitivity of the similarity, which increases the matching to some extent. In [6], the fuzzy feature is introduced into the shape context and the circular shift matching is employed to improve the retrieval precision. In addition, Cao et al. in 2008 present a new fuzzy shape context matching approach, in which a new coordinate is given to calculate point-feature images' local shape information histograms and the weighted sum of the cost of shape contexts for matching points and the cost of total feature matching is exploited as the similarity measure for matching [9]. It is successfully applied to the matching of infrared and visible image sequences. Besides the above shape context approaches that directly take full advantage of shape, there are a couple of indirect shape feature methods such as the path similarity skeleton graph matching presented in [14] and the hierarchical matching [15], both of which also have a better matching performance. In total, a variety of shape context approaches are continuously presented in recent years and significant advances are indeed achieved. But it still remains open problem in occurrence of partial missing or occlusion of object shape. The reason is that they may have great influence on matching precision.

In this paper, we first construct a rule-based fuzzy representation of shape context and then present a new multi-clue based fuzzy shape context approach (MFSC) using combination of geometric information and graph transduction. The MFSC takes complexity of object shape into account. In this approach, we specifically redefine the distance between arbitrary two sampled points on any shape and employ graph transduction to correct and compensate training error. Additionally, we propose a new fuzzy shape context approach that is based on both multi-clue and state reservoir computing. The experimental results demonstrate that the accuracy of detection achieved by the proposed approach on Kimia-216 and Kimia-99 benchmark datasets is up to 99.35% and 98.56%, respectively.

This work was supported in part by the National Science Foundation of China (NSFC) under Grant Nos. 90820305 and 60775040 and by the National High-Tech R & D Program of China under Grant No. 2012AA041402.

II. A New Fuzzy Shape Context Approach Based on Multi-clue and State Reservoir Computing

A. A rule-based fuzzy representation of shape context descriptor

While sampled points are projected using the standard shape context approach, there exist some problems. In fact, the quantization is rather accurate for the sampled points that are nearer to log-polar origin. But the quantization of the sampled point is just an approximation if it is far away from the origin. Thus the membership function and the fuzzy rule need to be adopted to correct the approximation error. As shown in Fig. 1, the point p is located at the bin A. But it is also very close to the bins of B, C, and D. We could regard the point p as belonging to the three bins to some extent. From this perspective, it is necessary to introduce fuzzy rules for shape matching.

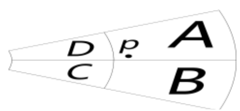

Fig. 1. The fuzzification of bin.

Considering that the projection of the sampled points on the shape context with respect to the origin is a 2D space about angle and log-distance, we could use the 2D membership function to describe the class of sampled points. The procedure of building fuzzy rules for shape context is given below.

Procedure 2.1: Let

$$S_r = \{\log R_m : m \text{ is an integer between 1 and } M, \text{ and } R_m \text{ is the } m\text{-th fuzzy partitioning level}\} \tag{1}$$

$$S_\theta = \{\frac{2\pi n}{N} : n \text{ is an integer between 1 and } N\} \tag{2}$$

where both $\triangle S_r = S_r - S_{r-1}$ and $\triangle S_\theta = S_\theta - S_{\theta-1}$ are constant.

Assume that the set of central points for each bin in histogram is indicated by $C = \{(\log r_m, \theta_n)\}$. It has

$$\log r_m = \left(\log R_m + \log R_{m-1}\right)/2, \cdots, \log r_1 = \log R_1/2 \tag{3}$$

$$\theta_n = \pi(2n-1)/N \tag{4}$$

Now let us give the definition of fuzzy membership function below. Suppose that $\mu_{\mathrm{m}}(\log r)$ and $\mu_{\mathrm{n}}(\theta)$ denote the membership function of log-distance and angle $(\log r, \theta)$, respectively, which correspond the sampled point p_i, with respective to the $(\log r_m, \theta_n)$. Without loss of generality, the bell-shaped membership function is adopted in this paper, i.e.,

$$\mu_m(\log r) = \begin{cases} f\left(\frac{r_m - r}{r_m - R_{m-1}}\right), & (R_{m-1} < r \le r_m,\ m \ge 2) \\ f\left(\frac{r - r_m}{R_m - r_m}\right), & (r_m < r \le R_m) \\ 1 - f\left(\frac{r - r_{m-1}}{R_{m-1} - r_{m-1}}\right), & (r_{m-1} < r \le R_{m-1},\ m \ge 2) \\ 1 - f\left(\frac{r_{m+1} - r}{r_{m+1} - R_m}\right), & (R_m < r \le r_{m+1},\ m < M) \\ 1 & (r \ge r_M \text{ or } r \le r_1 (M \text{ denotes the bin's level}) \\ 0, & \text{other} \end{cases} \tag{5}$$

where $f(x) = \exp(-x^2/2\sigma^2)$, and the value of σ is found according to the variance on all the points of each bin.

Due to $\Delta\theta = \theta_{n+1} - \theta_n = 2\pi/N$ being constant, the membership function of angle is define by

$$\mu_n(\theta) = \begin{cases} f\left(\frac{2(\theta - \theta_n)}{\Delta\theta}\right), & \left(\theta_n < \theta \le \theta_n + \frac{\Delta\theta}{2}\right) \\ f\left(\frac{2(\theta_n - \theta)}{\Delta\theta}\right), & \left(\theta_n - \frac{\Delta\theta}{2} < \theta \le \theta_n\right) \\ 1 - f\left(\frac{2(\theta_{n+1} - \theta)}{\Delta\theta}\right), & \left(\theta_n + \frac{\Delta\theta}{2} < \theta \le \theta_{n+1}\right) \\ 1 - f\left(\frac{2(\theta - \theta_{n-1})}{\Delta\theta}\right), & \left(\theta_{n-1} < \theta \le \theta_n - \frac{\Delta\theta}{2}\right) \\ 0, & \text{other} \end{cases} \tag{6}$$

Note that the fuzzy shape context approach presented in this paper uses the raw distance instead of log-distance as the input of the linguistic variable. This not only avoids statistical bias caused by scaling of object, but also ensures the effective use of fuzzy rules. We select the bell-shaped membership function for each of bins in histogram so as to facilitate the evaluation of variance on all the data projected on the bin. The fuzzy shape context histogram of Fig. 2(a) is shown in Fig. 2(b).

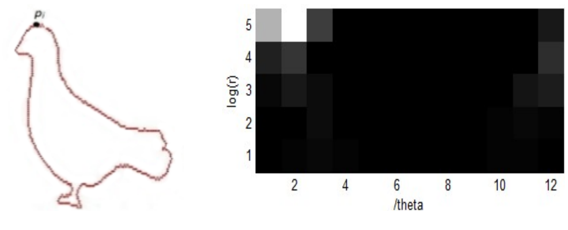

(a) (b)

Fig. 2. The original input image and its corresponding fuzzy shape context histogram.

B. A multi-clue based fuzzy shape matching algorithm

(1) A fuzzy shape matching algorithm based on graph transduction

Actually, there occur some classification mistakes in the standard shape context approach as dealing with the object with partially missing shape. For example, let us consider three object shapes contained in Kimia-99, as shown in Fig. 3. It is easy to see that the similarity of the cow on the left and the dog in the middle is larger than that of the dog in the middle and the dog on the right. To eliminate such classification mistakes, we need to add a new clue.

Fig. 3. Some examples of easily confused objects on Kimia-99.

In this paper, we utilize the graph transduction technique [5] and further combine with the Floyed-Warshall algorithm that computes the shortest path between any two points to update the affinity matrix. It is intended to resolve partial missing problems of object shape.

Procedure 2.2:

1) For all the objects that are pair-wisely matched based on the fuzzy shape context, evaluate the cost function D_{ij} ($j \neq i$).

2) For all the pair of points (u, v), find the cost function D_{uv}. If there exist an k ($k \neq u$ and $k \neq v$) such that it holds $D_{uk} + D_{kv} < D_{uv}$, then update D_{uv}, i.e., $D_{uv} = D_{uk} + D_{kv}$.

3) The similarity of the objects i and j is defined by $W_{i,j} = \mathrm{sim}(X_i, X_j)$. It is calculated by both the matching cost function $D_{i,j}$ for arbitrary two objects and the scaling factor $\sigma_{i,j}$ determined by an empirically-selected value α and the k-neighbor function coefficient k [13] (in this paper, we chose $\alpha = 0.4$ and $k = 5$). As a result, the probabilistic affinity matrix $P = \{P_{i,j}\}$ can be calculated, i.e.,

$$W_{i,j} = \exp\left(-\frac{D_{i,j}^2}{\sigma_{i,j}^2}\right), \quad P_{i,j} = \frac{W_{i,j}}{\sum_{k=1}^{n} W_{i,k}}. \tag{7}$$

4) Define $f(x_i)$ as the similarity of a classified object x_i and an unclassified object x_1. At the initial step, let $f(x_i) = \mathrm{sim}(x_i, x_j)$. In the process of graph transduction, the similarity of x_i and x_1 is updated by the following recursive equation,

$$f(x_i) = \sum_{j=1}^{n} P_{i,j}\, f(x_j). \tag{8}$$

5) Construct the time sequence $f_t(x_i)$ and set the initial condition as

$$f_1(x_1) = 1,\ f_1(x_i) = 0\ (i = 2,3,\cdots,n). \tag{9}$$

Given the upper time bound T and the threshold Δ, the iteration terminates if $t \geq T$ or for arbitrary time point t,

$$|f_{t+1}(x_i) - f_t(x_i)| < \Delta. \tag{10}$$

Consequently, the output $f(x_i)$ at this time step is used as the final result. Note that there remains $f_{t+1}(x_1) = 1$ during each of the iterations.

6) After evaluating $f(x_i)$, the maximum $f(x_m)$ among them is found. The object x_1 is then discriminated as the same class as x_m.

Compared to the graph transduction technique proposed by Bai *et al*. [5], which is similar to the PageRank algorithm, the shortest path between arbitrary two points is calculated in our approach. It not only reduces the number of iteration, but also improves the time efficiency.

(2) A fuzzy shape context algorithm of combining geometric clues.

In the standard shape context approach, the definition of distance between arbitrary two points on an object shape generally ignores geometric information between two points. In this paper, we use the line fitting algorithm and the graph algorithm to improve our shape context algorithm. First, we compute a slope of line segment between arbitrary adjacent points located on shape, then classify them according to the relationship between the slope and the points, and finally perform a line fitting. This implies that object contour is first transformed into polygon and then projected onto the histogram's bin according to the distance between arbitrary two points that is evaluated using the graph algorithm.

Procedure 2.3:

1) For the point set $P = \{ p_1, p_2, \cdots, p_\lambda\}$, calculate every slope K_i and intercept B_i of the line segment formed by arbitrary adjacent two points of p_i and p_{i+1} .

2) Set the slope threshold T_k ($T_k > 1$) and the intercept threshold T_b. For arbitrary i and j (let us assume $K_i > K_j$), p_i, p_{i+1}, p_j, p_{j+1} are regarded to belong to an identical set of line segments if $0 < K_i/K_j < T_k$ and $|B_i - B_j| < T_b$.

3) After yielding m sets of line segments, we fit all the points from each of the sets of line segments using RANSAC and form a polygon that approximates an object contour.

4) Let us denote the two ends of each line segment l_i ($1 \leq i \leq m$) by s_i and e_i and make records of all the sampled points that are used to fit the line l_i. The distance between sampled points p_a and p_b can be given below.

a) If p_a and p_b are on the same line, we then use the following Euclidean distance formula,

$$D_{ab} = \sqrt{(p_{ax} - p_{bx})^2 + (p_{ay} - p_{by})^2}. \tag{11}$$

b) If p_a and p_b are not on the same line, we could calculate the shortest distance between the two sampled points according to the adjacent relationship between the lines. Assume that the ends of the fitting lines that p_a and p_b belong to are indicated by (s_a, e_a) and (s_b, e_b), respectively. Using the shortest path algorithm (e.g., the Dijkstra algorithm), we first compute the shortest distance between these endpoint-pairs and then add up the distance between p_a (p_b) to its corresponding endpoint. Let us denote l_1 by the shortest path from s_a to s_b, l_2 by the one from s_a to e_b, l_3 by the one from e_a to s_b, and l_4 by the one from e_a to e_b. We have

$$D_{ab1} = \sqrt{(p_{ax} - p_{sax})^2 + (p_{ay} - p_{say})^2} + \sqrt{(p_{bx} - p_{sbx})^2 + (p_{by} - p_{sby})^2} + l_1 \tag{12}$$

$$D_{ab2} = \sqrt{(p_{ax} - p_{sax})^2 + (p_{ay} - p_{say})^2} + \sqrt{(p_{bx} - p_{ebx})^2 + (p_{by} - p_{eby})^2} + l_2 \tag{13}$$

$$D_{ab3} = \sqrt{(p_{ax} - p_{eax})^2 + (p_{ay} - p_{eay})^2} + \sqrt{(p_{bx} - p_{sbx})^2 + (p_{by} - p_{sby})^2} + l_3 \tag{14}$$

$$D_{ab4} = \sqrt{(p_{ax} - p_{eax})^2 + (p_{ay} - p_{eay})^2} + \sqrt{(p_{bx} - p_{ebx})^2 + (p_{by} - p_{eby})^2} + l_4 \tag{15}$$

$$D_{ab} = \min\{D_{ab1}, D_{ab2}, D_{ab3}, D_{ab4}\} \tag{16}$$

Actually, standard shape context approaches do not distinguish between the complex and simple objects. In their matching strategies, the similar procedures such as point extraction and histogram matching are often exploited. This is no necessary and may lead to the false detection. To address this problem, this paper introduces *priori* knowledge through adding the geometric information of object shape itself. For a closed curve, the ratio of perimeter's square and area, which is denoted by R, is in general viewed as an important measure to describe shape complexity. Thus we statistically computed the R values of all the classified objects contained in Kimia-216 and Kimia-99 datasets and validated the fact that the shape complexity for the same class of objects is totally very close, where the ratio of the minimum and the maximum for each of classes is greater than 0.7. In this way, it is required to carry out preprocessing for arbitrary two objects to be classified. It means that it is unlikely to be classified as the same class of objects if their shape complexity is greater than a certain threshold.

(3) A multi-clue based fuzzy shape matching algorithm using graph transduction and geometric information

This paper integrates both geometric information and graph transduction into the fuzzy shape context detection. Using the above-mentioned algorithm that combines the line fitting algorithm and the graph one, the distance between two sampled points can be found. In addition, the pair-wisely matching histogram cost function table for all the objects is evaluated and updated according to our graph transduction technique. Any two objects are not considered as belonging to the same class if the shape complexity ratio is greater than a certain threshold T (generally, the default value of T is set to 2). Eventually, we could have the final object detection through updating of the histogram cost function table with the geometric complexity.

C. A new fuzzy shape context approach based on both multi-clues and state reservoir computing

The known classes of object can be used as the training dataset in order to build an additional class detection template, while our multi-clue based fuzzy shape context approach (MFSC) is, as an initial step, employed to detect object. Considering that there exists shape or contour diversity for the same class of object, the detection of shape context is indeed a dynamic process. The SHESN neural network proposed in [16] generally has a better performance and a faster convergence as dealing with complex dynamic systems. In fact, the SHESN is suited well to the training of shape context due to the fact that the state reservoir of SHESN has powerful capabilities of dynamic memory.

In this paper, the Kimia-216 and Kimia-99 benchmark datasets are used as our training and test datasets. The Kimia-216 contains 18 classes, each class having 12 objects/pictures. We randomly pick up 6 pictures among 12 pictures each class so as to construct the training samples, and the remaining is chosen as the test samples. Similarly, the Kimia-99 includes 9 classes and 11 objects/pictures each class. The 5 pictures randomly selected from 11 pictures each class are used for the training and the rest is employed to build the test dataset.

For each picture/object in the training dataset, we extract 200 sampled points for an object shape. Consequently, the Kimia-216 (Kimia-99) has 1,200 (1,000) training input data each class, which leads to the 21,600 (11,000) training samples in total. Note that each of the training samples corresponds to a fuzzy histogram of one sampled point that contains 60 bins, as shown in Fig. 2(b). It means that each sample includes a 60-dimensional input vector. Meanwhile, the desired output is an n-dimensional vector, where n denotes the number of classes. For instance, n = 18 for Kimia-216 and n = 9 for Kimia-99. Specifically, only one element of the desired output vector that corresponds to an object class is set to 1 and all remaining ones are assigned to 0.

Let us take the Kimia-216 dataset as an example. The procedure for the training of SHESN network is described as follows:

1) Set up the state reservoir of SHESN. The capacity of state reservoir is selected as $200 \times 200 = 40{,}000$, the number of internal neurons is set to 500, the number of backbone neurons is 5, and the degree of local neurons is assigned as 5. The noise $v(k)$ is randomly generated using the uniform distribution over [-0.0008,0.0008], and the input weight matrix W^{in} and the feedback weight matrix W^{fb} are randomly produced with the uniform distribution over [-1,1]. According to the rules of [16] that generate the naturally evolving state reservoir, we produce the state reservoir of SHESN in a generative way.

2) All the 21,600 samples in the training dataset are given by

$$\{u(1), y_d(1); u(2), y_d(2); \cdots ;u(N), y_d(N)\},$$

where $u(k)$ ($k = 1,2,\cdots,21{,}600$) represents the input vector at the time step k, which is a 60-dimensional vector for the fuzzy shape context and $y_d(k)$ indicates the desired output. It corresponds to an 18-dimensional binary vector, in which only one element has 1.

3) The output weight matrix W^{out} of SHESN is updated with the above training dataset using the supervised learning algorithm such as the ridge regression.

4) After training with 21,600 samples, the learning process terminates.

Similarly, there are 200 sampled points for every object shape/picture. As the 60-dimensional input vector of SHESN, the fuzzy histogram for each sampled point should first be found using our MFSC approach.

The procedure for testing is summarized below:

1) 200 sampled points that correspond to each picture/object are added to the input vector and a new group of input-output pairs can be obtained by

$$\{u(m+1), y(m+1); u(m+2), y(m+2); \cdots ; u(m+200), y(m+200)\}.$$

2) For the outputs $y(m+i)$ (i=1,2,$\cdots$,200) that are produced with inputs of 200 sampled points each picture, we compute the averaging of $y(m+i)$, which is indicated by $Y(j)$ (j = 1, 2,$\cdots$,108). Note that we select 108 pictures from Kimia-216 dataset as the test samples.

3) Calculate the Euclidean distance between $Y(j)$ and the output vector that corresponds to 18 classes, and find the class that has the shortest path. The picture/object is thus discriminated as belonging to this class.

III. Experimental Results and Analysis

In our experiments, we exploited all the data from Kimia-99 and Kimia-216. The Kimia-99 dataset contained 9 classes, such as human being, cow, plane, and fish, each class having 11 samples/pictures. The Kimia-216 included 18 classes and 12 samples/pictures each class [13]. In this paper, we first conducted an extensive comparative study of the proposed multi-clue based fuzzy shape context approach (MFSC) with the standard shape context (SC) [1], the generative model (GM) [11], the inner-distance shape context (IDSC) [4], and the circular shift fuzzy shape context approach (FSC+SCS) [6]. On the Kimia-216 and Kimia-99 datasets, the detection results achieved are listed in Table I and Table II, respectively.

TABLE I. THE DETECTION RESULTS ON KIMIA-216

Approach	1st	2nd	3rd	4th	5th	6th	7th	8th	9th	10th	Sum	Avg
SC[1]	214	209	205	197	191	178	161	144	131	101	1731	80.14%
FSC+SCS[6]	216	216	215	214	213	213	209	203	191	188	2078	96.20%
MFSC	216	216	215	214	211	206	203	191	185	177	2034	94.17%

TABLE II. THE DETECTION RESULTS ON KIMIA-99

Approach	1st	2nd	3rd	4th	5th	6th	7th	8th	9th	10th	Sum	Avg
SC[1]	97	91	88	85	84	77	75	66	56	37	756	76.36%
GM[11]	99	97	99	98	96	96	94	83	75	48	885	89.39%
IDSC[4]	99	99	99	98	98	97	97	98	94	79	958	96.76%
FSC+SCS[6]	99	99	99	99	99	99	98	95	94	91	972	98.18%
MFSC	99	99	99	99	97	98	96	94	93	90	964	97.37%

Fig. 4 and Fig. 5 further give the A-R curves obtained using our MFSC approach and the standard shape context approach on Kimia-216 and Kimia-99 datasets, respectively. It was readily observed from Tables I-II and Figs. 4-5 that the detection accuracy of the MFSC was significantly improved, compared to all the standard shape context approach, the generative model, and the inner-distance algorithm. But it was slightly inferior to that of the circular shift fuzzy shape context approach presented in [6].

We thus used our fuzzy shape context approach based on both multi-clues and SHESN to fulfill performance evaluation and comparative study on the object shape databases of Kimia-216 and Kimia-99, respectively. The experimental results show that the proposed approach can have the detection accuracy of up to 99.35% and 98.56%, respectively, on the above two benchmark datasets.

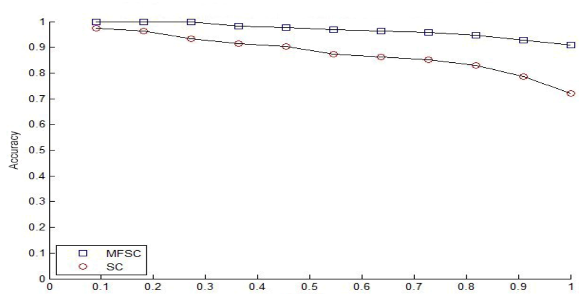

Fig. 4. The A-R curves on Kimia-216.

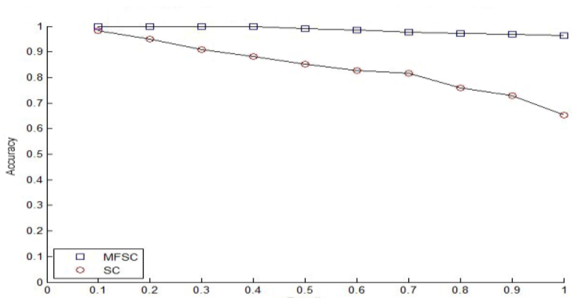

Fig. 5. The A-R curves on Kimia-99.

IV. CONCLUSION

This paper investigates a fuzzy shape context approach for visual object recognition using both multi-clues and reservoir computing. We combine fuzzy representation, geometric clue, graph transduction, and reservoir computing to improve traditional shape context approaches. Furthermore, the effectiveness and efficiency of the proposed approach are validated on standard object shape datasets, achieving satisfying experimental results. Using Kimia-216 and Kimia-99 datasets, the detection accuracy of the fuzzy shape context approach that combines multi-clues with SHESN model can reach up to 99.35% and 98.56%, respectively, all of which outperform that of the state-of-the-art shape context approaches.

REFERENCES

[1] S. Belongie, J. Malik, and J. Puzicha, "Shape matching and object recognition using shape contexts," IEEE Trans. Pattern Analysis and Machine Intelligence, vol. 24, no. 24, pp. 509–522, April 2002.

[2] S. Belongie, J. Malik, and J. Puzicha, "Shape context: a new descriptor for shape matching and object recognition," Advances in Neural Information Processing System 13, Proc. 2000 Conf., T. K. Leen, T. G. Dietterich, and V. Tresp, eds., pp. 831–837, 2001.

[3] G. Mori, S. Belongie, and J. Malik, "Efficient shape matching using shape contexts," IEEE Trans. Pattern Analysis and Machine Intelligence, vol. 11, no. 27, pp. 1832–1837, November 2005.

[4] H. Ling and D. W. Jacobs, "Shape classification using the inner-distance," IEEE Trans. Pattern Analysis and Machine Intelligence, vol. 29, no. 2, pp. 286–299, February 2007.

[5] X. Bai, X. Yang, L. J. Latecki, W. Liu, and Z. Tu, "Learning context-sensitive shape similarity by graph transduction," IEEE Trans. Pattern Analysis and Machine Intelligence, vol. 32, no. 5, pp. 861–874, May 2010.

[6] M. Han and D. Zheng, "Shape recognition based on fuzzy shape context," Acta Automatica Sinica, vol. 38, no. 1, pp. 68–75, January 2012. (in Chinese)

[7] X. Ding, H. Wu, H. Zhang, and S. Ma, "Review on shape matching," Acta Automatica Sinica, vol. 27, no. 5, pp. 678–694, May 2001. (in Chinese)

[8] Y. Zhou, J. Liu, and X. Bai, "Research and perspective on shape matching," Acta Automatica Sinica, vol. 38, no. 6, pp. 889–910, June 2012. (in Chinese)

[9] Z. Cao, R. Yan, and Z. Song, "Approach on fuzzy shape context matching between infrared images and visible images," Infrared and Laser Engineering, vol. 37, no. 6, pp. 1095–1100, December 2008. (in Chinese)

[10] X. Shu and X. Wu, “A novel contour descriptor for 2D shape matching and its application to image retrieval,” Image and Vision Computing, vol. 29, no. 4, pp. 286–294, March 2011.

[11] Z. Tu and A. L. Yuille, “Shape matching and recognition-using generative models and informative features,” Proceedings of the 8th European Conference on Computer Vision, pp. 195–209, May 2004.

[12] F. Wang, J. Wang, C. Zhang, and H. Shen, “Semi-supervised classification using linear neighborhood propagation,” Proc. IEEE Conf. Computer Vision and Pattern Recognition, June 2006.

[13] T. B. Sebastian, P. N. Klein, and B. B. Kimia, “Recognition of shapes by editing their shock graphs,” IEEE Trans. Pattern Analysis and Machine Intelligence, vol. 26, no. 5, pp. 550–571, May 2004.

[14] X. Bai and L. J. Latecki, “Path similarity skeleton graph matching,” IEEE Trans. Pattern Analysis and Machine Intelligence, vol. 30, no. 7, pp. 1282–1292, July 2008.

[15] P. F. Felzenszwalb and J. D. Schwartz, “Hierarchical matching of deformable shapes,” In: Proceedings of the 2007 IEEE Conf. Computer Vision and Pattern Recognition, pp. 1–8, June 2007.

[16] Z. D. Deng and Y. Zhang, “Collective behavior of a small-world recurrent neural system with scale-free distribution,” IEEE Trans. Neural Networks, vol. 18, no. 5, pp. 1364–1375, September 2007.